J. Shanghai Jiao Tong Univ. (Sci.), 2019, 24(5): 571-578
https://doi.org/10.1007/s12204-019-2115-1

Research and Implementation of Beidou-3 Satellite Multi-Band Signal Acquisition and Tracking Method

CHEN Shuhao (陈树浩), *MAO Xuchu** (茅旭初)
(School of Electronic Information and Electrical Engineering, Shanghai Jiao Tong University, Shanghai 200240, China)

Abstract: A new acquisition and tracking method is proposed for signal processing under the new signal system structure of Beidou-3 navigation satellite system (BDS-3). By starting with the analysis of the characteristics and signal structure of the new signal, the local replica of the ranging code and the study of the characteristics of the ranging code are completed, which proves that the method in this paper can be used in the subsequent acquisition and tracking process. The fast Fourier transformation (FFT) search based on longer coherence time and the adaptive phase-frequency switching carrier tracking loop are proposed for signals in different modulation modes. The actual signal of Beidou-3 satellite is sampled by local experiment, and the acquisition and tracking of the Beidou-3 satellite multi-band signal is finally completed. The tracking results verify the feasibility of the proposed acquisition and tracking method.

Key words: Beidou-3 navigation satellite system (BDS-3), binary offset carrier (BOC), B1C signal, B3I signal, acquisition and tracking method
CLC number: TN 967.1 **Document code:** A

0 Introduction

Beidou navigation satellite system (BDS), as one of the global navigation satellite systems (GNSSs), is a steadily promoting construction in accordance with the development strategy. In order to achieve global coverage and better service to the needs of users in China and around the world, Beidou-3 navigation satellite system (BDS-3) has been developing and establishing now. With the acceleration of the construction of BDS-3, its demand and application market will rapidly expand and develop. Therefore, as the basis for incorporating BDS-3 into user applications, the acquisition and tracking of B1C and B3I signals with better performance in BDS-3 has become a crucial research content. By 2020, BDS-3 will form a 30-satellite constellation including 3 geostationary orbit (GEO) satellites, 3 inclined geosynchronous orbit (IGSO) satellites and 24 medium-earth orbiting (MEO) satellites, providing open, free, high-quality positioning, navigation, timing, search and rescue, as well as short messages and many other services to users around the world[1-2].

From November 5, 2017 to August 31, 2018, BDS-3 had launched 12 satellites which are all MEO satellites. Compared with Beidou-2 navigation satellite system (BDS-2), BDS-3 uses more advanced technology. Firstly, the performance, satellite life and service accuracy of the system are better than those of BDS-2. Secondly, the scale of construction is larger; the number of Beidou-3 satellites is doubled as compared with that of Beidou-2 satellites. Thirdly, the functions of BDS-3 are stronger, increasing the inter-satellite links and forming a complex system of satellite networking, which greatly enhances the level of integration of the system. Meanwhile, BDS-3 increases interoperable signals which have better performance; especially in the B1C signal, the signal modulation mode and the way that the ranging code is generated are changed, so that it can still be used independently within the GPS common frequency band. In addition, higher-performance cesium atomic clock and hydrogen atomic clock are used on the satellite. The cesium atomic clock stability is E-14 level, and the hydrogen atomic clock stability is E-15 level. By adopting new technology, the spatial signal accuracy is better than 0.5 m, and the positioning accuracy is increased by 1—2 times to a level of 2.5—5 m[3].

With the acceleration of the construction of BDS-3, its demand and application market also rapidly expand and develop. Therefore, as the basis for incorporating BDS-3 into the user application, the acquisition and tracking of the newly-operated interoperable B1C and B3I signals in Beidou-3 satellites, that is, the signal processing part, has become a crucial content. Because Beidou-3 satellites are just put into use and new signals

Received date: 2018-10-28
∗**E-mail:** maoxc@sjtu.edu.cn

are added, there is little research on the acquisition and tracking method of these new signals. In this paper, the signal structure is analyzed, and an improved acquisition and tracking method is proposed. In addition, this study can provide a theoretical basis for the use of BDS-3 and make preparation for the global network of BDS-3 in the future. It can accelerate the deep integration between Beidou satellite positioning navigation and various industries. Meanwhile, it can also fill the gap of the current research on BDS-3 signal processing[4], which possesses strong novelty and strategic significance.

1 Characteristics and Structure of B1C and B3I Signals of Beidou-3 Satellite

Different structural characteristics and modulation techniques are used into the Beidou-3 satellite signals due to frequency band sharing, so the characteristics and modulation techniques are introduced at first. Then the characteristics of the modulation technology applied to the corresponding Beidou-3 satellite signals are analyzed, and the local replica of the ranging code is completed.

1.1 Characteristics and Structure of B1C Signal

The basic characteristics of the Beidou-3 B1C signal are shown in Table 1, disclosed from the Beidou official document.

Table 1 Basic characteristics of the BDS-3 B1C frequency signal

Signal parameter	Description
Frequency	32.736 MHz bandwidth with a center frequency of 1 575.42 MHz
Modulation method	Data component: binary offset carrier technology, BOC(1, 1); Pilot component: quadrature multiplexed binary offset carrier technology, QMBOC(6, 1, 4/33)
Ranging code rate	1.023 megacycles per second
Chip length of primary code	10 230
Symbol rate	Data component: 100 samples per second; Pilot component: 0
Multiplexing mode	Code division multiple access (CDMA)
Polarization	Right-handed circular polarization (RHCP)

The B1C signal is composed of a data component and a pilot component. The data component is modulated by the navigation message and the ranging code through the subcarrier, in which a sinusoidal BOC(1, 1) modulation method is adopted. The pilot component is determined by the ranging code through the subcarriers, in which QMBOC(6, 1, 4/33) modulation mode is adopted. The power ratio of data component to pilot component is $1:3$.

The B1C signal expression is

$$S_X(t)=[s_{\mathrm{d}}(t)\cos(2\pi f_X t)- s_{\mathrm{p}}(t)\sin(2\pi f_X t)]\sqrt{2P_X}, \quad (1)$$

where P_X is the signal power, f_X is the signal carrier frequency, $s_{\mathrm{d}}(t)$ is the data component, and $s_{\mathrm{p}}(t)$ is the pilot component.

The expression of $s_{\mathrm{d}}(t)$ is

$$s_{\mathrm{d}}(t)=\frac{1}{2}D_{\mathrm{d}}(t)C_{\mathrm{d}}(t)c_{\mathrm{d}}(t), \quad (2)$$

where $D_{\mathrm{d}}(t)$ is the navigation message data, $C_{\mathrm{d}}(t)$ is the ranging code of data component, and $c_{\mathrm{d}}(t)$ is the subcarrier of data component. The expression of $c_{\mathrm{d}}(t)$ is

$$c_{\mathrm{d}}(t)=\mathrm{sign}(\sin(2\pi f_{\mathrm{a}}t)), \quad (3)$$

where f_{a} is 1.023 MHz.

The expression of $s_{\mathrm{p}}(t)$ is

$$s_{\mathrm{p}}(t)=\frac{\sqrt{3}}{2}C_{\mathrm{p}}(t)c_{\mathrm{p}}(t), \quad (4)$$

where $C_{\mathrm{p}}(t)$ and $c_{\mathrm{p}}(t)$ are the ranging code and subcarrier of pilot component, respectively. The pilot component subcarrier is a QMBOC(6, 1, 4/33) composite subcarrier, consisting of mutually orthogonal BOC(1, 1) subcarrier and BOC(6, 1) subcarrier, and the power ratio of the two subcarriers is $29:4$. The expression of $c_{\mathrm{p}}(t)$ is

$$c_{\mathrm{p}}(t)=\sqrt{\frac{29}{33}}\mathrm{sign}(\sin(2\pi f_{\mathrm{a}}t))- \mathrm{j}\sqrt{\frac{4}{33}}\mathrm{sign}(\sin(2\pi f_{\mathrm{b}}t)), \quad (5)$$

where f_{b} is 6.138 MHz.

1.2 Characteristics and Structure of B3I Signal

The basic characteristics of the BDS-3 B3I signal are shown in Table 2, disclosed from the Beidou official document.

The B3I signal is modulated on the carrier by the method of "ranging code plus navigation message". Its signal expression is

$$S^j_{\mathrm{B3I}}(t)=A_{\mathrm{B3I}}C^j_{\mathrm{B3I}}(t)D^j_{\mathrm{B3I}}(t)\cos(2\pi f_3 t+\varphi^j_{\mathrm{B3I}}), \quad (6)$$

where the upper corner symbol j is the satellite number, A_{B3I} is the B3I signal amplitude, C_{B3I} is the B3I signal ranging code, D_{B3I} is the data code modulated on the B3I signal ranging code, f_3 is the B3I signal carrier frequency, and φ_{B3I} is the B3I signal carrier phase.

It can be seen from Table 2 and Eq. (6) that the modulation method used by the B3I signal and the method of generating the ranging code are similar to those of the B2I signal which is commonly used by BDS-2. Therefore, it is not introduced too much in this paper, and we only show the results of its acquisition and tracking.

Table 2 Basic characteristics of the BDS-3 B3I frequency signal

Signal parameter	Description
Frequency	20.46 MHz bandwidth with a center frequency of 1 268.52 MHz
Modulation method	Binary phase shift keying (BPSK)
Ranging code rate	10.23 megacycles per second
Chip length of primary code	10 230
Data code rate	GEO satellite: 500 bit/s; MEO/IGSO satellite: 50 bit/s
Multiplexing mode	CDMA
Polarization	RHCP

1.3 BOC Modulation of B1C Signal

It is different from the previous phase shift keying modulation method that the BDS-3 B1C signal is modulated by binary offset carrier (BOC).

BOC modulation was first proposed by Betz, and its core is the multiplication of a pseudo-random code sequence with a sinusoidal subcarrier. Usually, BOC modulation can be expressed as

$$\mathrm{BOC}(m_\mathrm{s}, n_\mathrm{c}), \quad m_\mathrm{s} = \frac{f_\mathrm{s}}{f_\mathrm{ref}}, \quad n_\mathrm{c} = \frac{f_\mathrm{c}}{f_\mathrm{ref}}, \tag{7}$$

where f_ref is 1.023 MHz[5], f_s is the rectangular subcarrier frequency, and f_c is the spreading code rate.

With two variable parameters of f_s and f_c, BOC technology can freely distribute the signal energy in a specified part of the signal bandwidth to reduce the interference when receiving other signals[6]. Due to the unique splitting characteristics of power spectra, the frequency band can share with GPS L1 frequency band, which is precious in the present conditions that the good frequency band is scarce[7]. However, due to the existence of subcarriers, it is difficult to adopt BPSK modulated signals in the tracking of BOC signals, especially for the high-order BOC signals, because the divergence caused by subcarriers can lead to shifting between BPSK correlation peaks and sine waves and cause tracking inaccuracy[8].

2 Generating the Local Ranging Code of B1C Signal

The premise of the signal acquisition and tracking is to complete the local replica of the ranging code. This section mainly introduces the method of generating a ranging code for the new B1C signal.

The ranging code of the B1C signal adopts a layered-code structure, consisting of a primary code and a secondary code. The starting time of the secondary code chip is strictly aligned with the starting time of the first chip of the primary code, and the chip width of the secondary code corresponds to the period of the primary code. For the MEO and IGSO satellites, each satellite has a unique ranging code number corresponding to its pseudo-random noise (PRN) number.

The parameters of the B1C signal ranging code are shown in Table 3.

Table 3 Ranging code parameters of the BDS-3 B1C frequency signal

Signal component	Primary code type	Chip length of primary code	Primary code period/ms	Secondary code type	Chip length of secondary code	Secondary code period/s
B1C data component	Truncated Weil	10 230	10	–	–	–
B1C pilot component	Truncated Weil	10 230	10	Truncated Weil	1 800	18

Note: the B1C data component contains no secondary code.

Since the generation method of the data component of the B1C signal is also truncated by the Weil code like the generation method of the pilot component. Therefore, we only introduce the generation method of the B1C data component code.

Firstly, it is necessary to obtain a Weil code sequence with a code length of N. The Weil code has good correlation performance and has a relatively flexible optional sequence length[9]. The expression of the Weil code is

$$W(k; w) = L(k) \oplus L((k + w) \bmod N), \quad k = 0, 1, \cdots, N-1, \tag{8}$$

where $L(k)$ is the Legendre sequence with a code length of N, w is the phase difference between two Legendre sequences, and mod is a modular division operation. The expression of the Legendre sequence is

$$L(k) = \begin{cases} 1, & k \neq 0 \text{ and } k = Y^2 \bmod N \\ 0, & \text{other} \end{cases}, \tag{9}$$

where Y is an integer which makes $k = Y^2 \bmod N$. The Weil code sequence with a code length of N is cyclically intercepted to obtain a ranging code with a length of N_0. The expression of the ranging code with a length of N_0 is

$$c(n_\mathrm{r}; w; p) = W((n_\mathrm{r} + p - 1) \bmod N; w), \quad n_\mathrm{r} = 0, 1, \cdots, N_0 - 1, \tag{10}$$

where p is the intercept point, i.e., the Weil code is intercepted from the p point whose value ranges from 1 to N.

Then the local replica of the ranging code is obtained by the data mapping of $0 \to 1$ and $1 \to -1$. The rate of the B1C signal primary code is 1.023 megacycles per second, and the chip length of the code is 10 230 which is truncated by the Weil code with a chip length of 10 243. There are 63 primary codes for the B1C signal data component. The autocorrelation characteristics of the data component primary code with PRN 29 are shown in Fig. 1, where s_{cp} represents the code phase in the number of samples and n_{cp} represents the correlation peaks. The primary code cross-correlation characteristics between PRN 29 and PRN 30 are shown in Fig. 2.

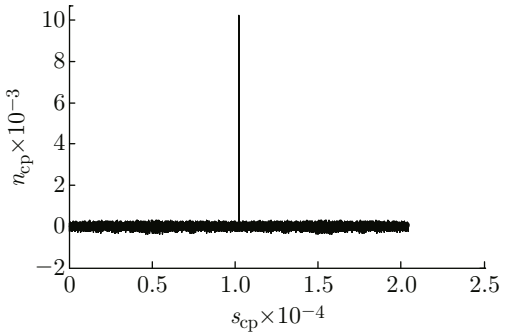

Fig. 1 Autocorrelation property of data component code with PRN 29

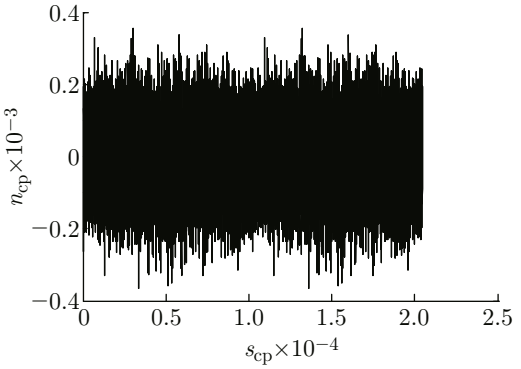

Fig. 2 Cross-correlation property of data component code between PRN 29 and PRN 30

It can be seen from Figs. 1 and 2 that the autocorrelation and cross-correlation properties of the B1C signal primary code are consistent with the characteristics of the conventional satellite ranging code.

3 Frequency-Domain Fast Fourier Transformation (FFT) Search Based on Longer Coherence Time

The data of Beidou-3 satellite signals used in this paper is collected by the data acquisition system which includes a seven-band measurement antenna, Beidou-3 data sampler, a 30 m low-loss radio-frequency (RF) connection cable, a USB3.0 conversion line and a computer for recording experimental data. The antenna is erected on the top of the SEIEE Group Building-2 of Shanghai Jiao Tong University.

After receiving the B1C signal data of Beidou-3 statellite, the acquisition process can be roughly summarized as follows: getting the received PRN code of the satellite, and then sequentially shifting the phase of the local replica of the ranging code with the PRN code of the satellite. The correlation operation is performed when the maximum value occurs, representing that the local replica of the ranging code matches the PRN code transmitted by the satellite, and the remaining phase should have a minimum value. In order to acquire satellite signals, it is necessary to get the carrier frequency of the satellite, and the Doppler shift needs to be considered because of the relative motion of the satellite and the Earth. Generally, the Doppler shift of the B1C signal is ±4 kHz, and the frequency shift of the PRN code is relatively small, so can be ignored. In summary, the acquisition of the B1C signal requires searching in a two-dimensional space composed of Doppler shift and chip phase. The most common and simplest method is time-domain serial search, but since the B1C signal uses BOC modulation, its multi-peak characteristic increases the probability of false acquisition. Therefore, it is necessary to increase the sampling frequency, which is equivalent to increasing the number of sampling points[10]. Under the premise that the time-domain serial search method has a large amount of computation, the search method needs to be improved to accelerate the operation speed. Therefore, the frequency-domain FFT search is usually used because of its higher acquisition speed. In previous studies[11], its acquisition speed can be increased by 8 times as compared with the time-domain serial search. The frequency-domain FFT search based on longer coherence time is proposed in this paper. The theoretical basis of this method is that a long sequence of discrete Fourier transforms can be decomposed into short-sequence discrete Fourier transforms, i.e., the original time-domain correlation operation can be replaced by frequency-domain FFT circular convolution operation.

The circular convolution formula can be expressed as

$$c_{xy}(m) = \sum_{n=-\infty}^{+\infty} x(n)y(m-n) = x(n) \oplus y(n), \tag{11}$$

where $x(n)$ is the acquired B1C signal code, and $y(n)$ is the local replica of the ranging code.

The above equation is subjected to Fourier

transform[12]:

$$R[m] = c_{xy}(m) = x(n) \oplus y(n) = F^{-1}[F(x(n))F(y(n))^*], \quad (12)$$

where $F^{-1}(\cdot)$ represents the inverse FFT (IFFT) operation, and $F(\cdot)$ represents the FFT operation.

The principle of the frequency-domain FFT search method is shown in Fig. 3.

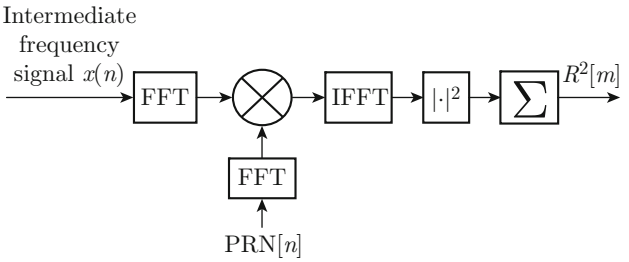

Fig. 3 FFT search block diagram

The obtained correlation value is compared with a preset threshold value, and if it is greater than the threshold value, the acquisition is successful. In this paper, the threshold is set to 4 times the average value of the correlation value, which is equivalent to an amplitude detection threshold of 6 dB[13].

The real BDS-3 B1C signal was acquired and processed on the MATLAB platform, and the PRN 29 satellite signal was successfully acquired, as shown in Fig. 4. Because the B1C signal is only transmitted on the Beidou-3 satellite and the number of Beidou-3 satellites is currently small, only one is acquired as a normal phenomenon. In Fig. 4, n_{icp} represents the immediate correlation peaks.

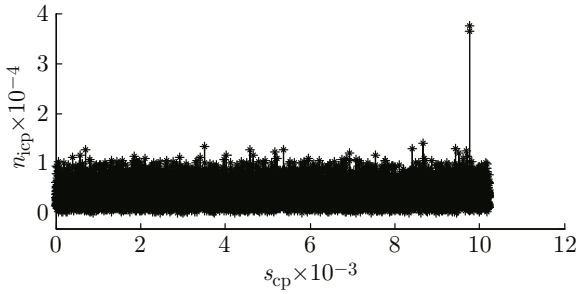

Fig. 4 B1C signal searching result of PRN 29 satellite

The BDS-3 B3I signals of PRN 3, PRN 7, PRN 10, PRN 18 and PRN 19 satellites were successfully acquired. The result of PRN 19 satellite is shown in Fig. 5.

From Figs. 4 and 5, the Beidou-3 satellite signals in the B1C frequency band and the B3I frequency band can be successfully acquired by the method of frequency-domain FFT search based on longer coherence time, which lays a foundation for the following tracking.

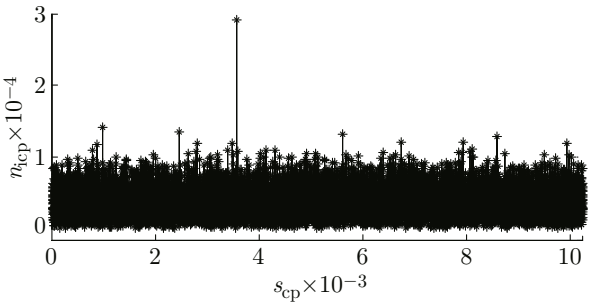

Fig. 5 B3I signal searching result of PRN 19 satellite

4 Tracking Method Based on Adaptive Phase-Frequency Switching Carrier Tracking Loop

The Beidou-3 statellite signal tracking is based on the successful acquisition which gets the code phase and the estimated value of the carrier Doppler shift, and then the carrier signal and useful data can be extracted. This part is mainly composed of two loops: the carrier tracking loop, and the code tracking loop. After these two loops stripping the carrier and pseudo code, the navigation message can be demodulated.

4.1 Adaptive Phase-Frequency Switching Carrier Tracking Loop

When the acquisition is completed, the ranging code has been basically synchronized, but due to the influence of Doppler shift and multipath effect, there is a frequency difference between the local carrier frequency and the carrier of the signal. In order to track the carrier accurately, it is necessary to obtain the frequency difference. The carrier tracking loop mainly includes two parts: a frequency-locked loop (FLL), and a phase-locked loop (PLL). The schematic diagram of the FLL is shown in Fig. 6[6], in which $f_1(t)$ represents the input code and $f_2(t)$ represents the output code.

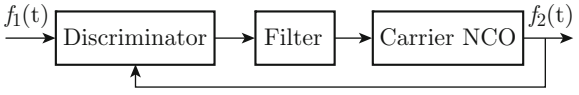

Fig. 6 Frequency locked loop principle[6]

In this paper, a cross product discriminator is used and its expression is

$$\Delta f_k = I(k-1)Q(k) - I(k)Q(k-1), \quad (13)$$

where

$$I(k) = AD(k)\mathrm{PN}(k)\sin\phi_k,$$
$$Q(k) = AD(k)\mathrm{PN}(k)\cos\phi_k,$$
$$\phi_k = \omega_{\mathrm{d}}T_k + \theta_0,$$

A is the signal amplitude, $D(k)$ is the modulation data, $\mathrm{PN}(k)$ is the PRN code, ω_{d} is the Doppler shift, T_k is

the code period, and θ_0 is the initial phase. The above formula can be rewritten as

$$\begin{aligned}\Delta f_k = &[AD(k)\mathrm{PN}(k)\cos\phi_k]\times\\ &[AD(k-1)\mathrm{PN}(k-1)\sin\phi_{k-1}]-\\ &[AD(k-1)\mathrm{PN}(k-1)\cos\phi_{k-1}]\times\\ &[AD(k)\mathrm{PN}(k)\sin\phi_k]=\\ &A^2D(k)D(k-1)R(\tau)\sin(\phi_k-\phi_{k-1}),\end{aligned}\tag{14}$$

where $R(\tau)$ is a value associated with $\mathrm{PN}(k)\mathrm{PN}(k-1)$.

When the continuously measured output data is constant, $D(k)D(k-1)=1$; when $|\omega_\mathrm{d}\pi T|\ll\pi/2$, $\sin(\phi_k-\phi_{k-1})\approx\phi_k-\phi_{k-1}$, where T is an entire cycle. Therefore, the output is proportional to the phase change of the unit time, so that the output numerically-controlled oscillator (NCO) can be used to control the carrier frequency to achieve the frequency tracking effect.

In order to eliminate the influence of symbol on the output in the experiment, a signed cross product discriminator is used and its expression is

$$\begin{aligned}\Delta f_k = &[I(k-1)Q(k)-I(k)Q(k-1)]\times\\ &\mathrm{sign}[I(k-1)I(k)+Q(k-1)Q(k)].\end{aligned}\tag{15}$$

The loop after the discriminator of Fig. 6 is changed to the phase detector is the PLL schematic. Its phase discrimination expression is

$$\Delta\phi_k=\arctan\left(Q_k/I_k\right).\tag{16}$$

In the general carrier loop, the PLL and the FLL operate independently. However, there is more data due to the longer coherence time in the acquisition phase. These two independently operating loops require more memory and time. Therefore, the adaptive phase-frequency switching method, proposed in this paper, can greatly reduce the carrier tracking time without losing the carrier tracking effect. The specific method is firstly to set a frequency difference threshold and then perform FLL tracking to reduce the Doppler frequency difference as soon as possible. When the frequency difference is less than the threshold value, the Doppler frequency difference is basically stripped and then the accurate tracking through the PLL can be done. Using this method, the signal tracking time can be effectively shortened, especially in the BOC modulated signal tracking or weak signal tracking that needs to be performed for longer coherence time.

4.2 Integrated Code Tracking Loop

Since the B1C signal is modulated by BOC, we design an integrated code tracking loop to integrate the BOC modulation subcarrier with the ranging code. Firstly, the local subcarrier performs XOR with the ranging code, and then puts the output into code tracking loop[14]. The integrated code tracking loop is mainly composed of a code ring discriminator, a filter and a ranging code NCO and a subcarrier NCO.

The code circle discriminator uses the commonly used early-minus-late (EML) discriminator. The core idea is to correlate signals with the three local replicas of the ranging code (early, prompt and late) to obtain three correlation values (I_E, I_P and I_L, respectively) and then get the discriminator output according to the correlation value. The expression of the discriminator output is

$$o_\mathrm{d}=\frac{|I_\mathrm{E}|-|I_\mathrm{L}|}{|I_\mathrm{E}|+|I_\mathrm{L}|}.\tag{17}$$

The loop uses a first-order low-pass filter to filter out unwanted high frequencies and noise in the output. The transfer function can be expressed as

$$\begin{aligned}F_\tau(s)=\frac{\sqrt{2}w_\mathrm{n}s+w_\mathrm{n}^2}{K_\mathrm{d}K_\mathrm{v}s}=\frac{1}{K_\mathrm{d}K_\mathrm{v}}\left(\sqrt{2}w_\mathrm{n}+w_\mathrm{n}^2s^{-1}\right)=\\ \frac{1}{K}\left(\sqrt{2}w_\mathrm{n}+w_\mathrm{n}^2s^{-1}\right),\end{aligned}\tag{18}$$

where K_d is the discriminator gain, K_v is the code ring oscillator gain, and ω_n is the angular frequency.

The flow chart of the tracking method is shown in Fig. 7.

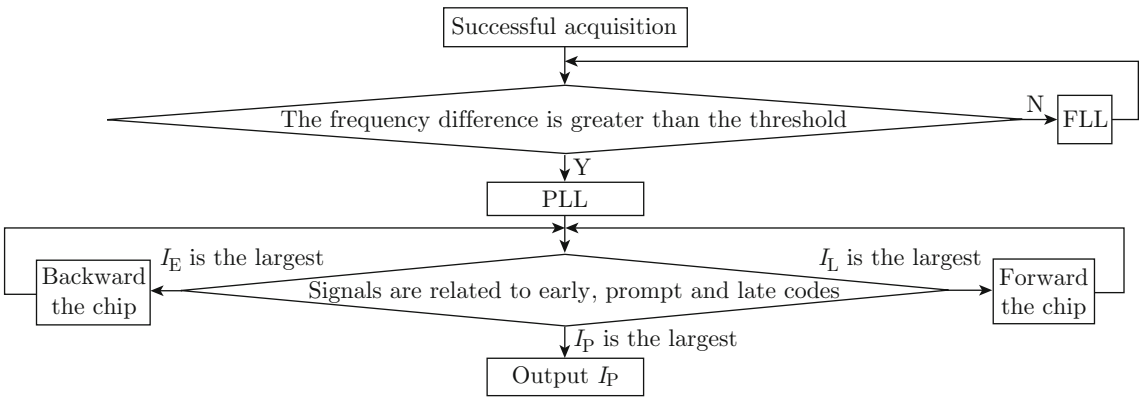

Fig. 7 Flow chart of the tracking method

After completing above tracking loop, the tracking result of the B1C signal of PRN 29 satellite is shown in Fig. 8. The former four hundred points are coarse tracking process of the FLL, followed by accurate tracking process of the PLL.

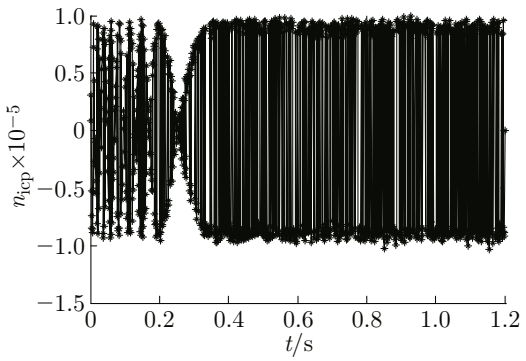

Fig. 8 B1C signal tracking result of PRN 29 satellite

The detail of the immediate correlation peaks from 400 to 550 ms is shown in Fig. 9.

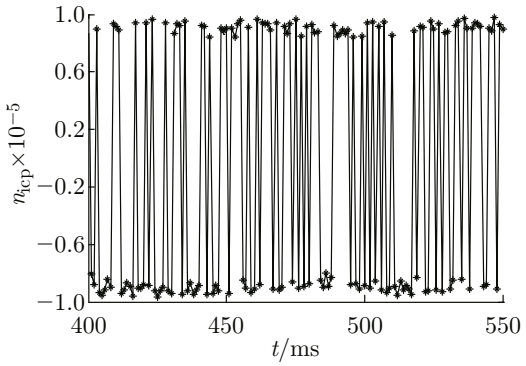

Fig. 9 B1C signal tracking detail of PRN 29 satellite

It can be seen from Fig. 9 that the correlation values of the positive and negative polarities are distinct and substantially linear.

The tracking result of PRN 19 satellite is shown in Fig. 10 and the detail of the B3I signal from 400 to 550 ms is shown in Fig. 11.

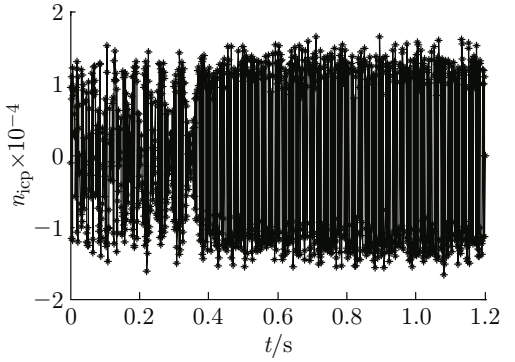

Fig. 10 B3I signal tracking result of PRN 19 satellite

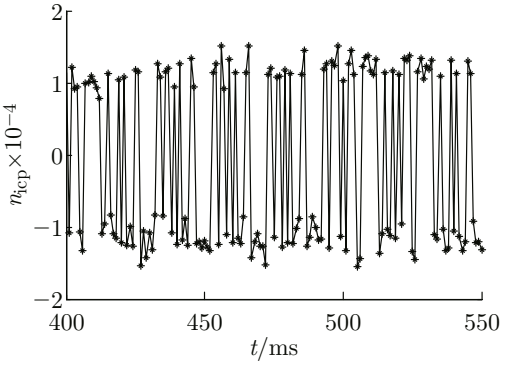

Fig. 11 B3I signal tracking detail of PRN 19 satellite

4.3 Verification and Analysis of Tracking Result

In order to verify the correctness of the tracking result, the tracking result can be correlated with the secondary code of the pilot component. Because each PRN satellite corresponds to a different secondary code of the pilot component, and the tracking result of the satellite is modulated by the secondary code of the pilot component, if there is a maximum value, the tracking result and the secondary code are in agreement, i.e., the tracking result is successful. The tracking result of the B1C signal of PRN 29 satellite is verified, as shown in Fig. 12.

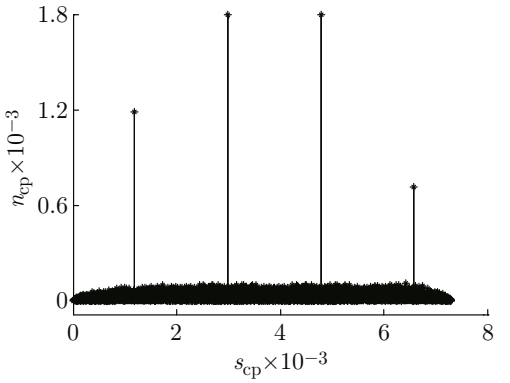

Fig. 12 Verification of B1C signal tracking result of PRN 29 satellite

It can be seen from Fig. 12 that since the chip length of the secondary code is 1 800, the correlation operation starts from the former 1 800 points to the last 1 800 points, and every set of 1 800 points as a period. There is a maximum correlation value appears in each period, confirming that the proposed method can accurately acquire and track the Beidou-3 satellite signals.

As mentioned above, in the general carrier loop method, the PLL and the FLL operate independently. This paper proposes the adaptive phase-frequency switching method. The general carrier loop method and the proposed method are compared in the same

hardware and device environment. The comparing results are shown in Table 4, where t_{ot} represents the time consumption for traversing the overall tracking of all satellites.

Table 4 The comparing results of two methods

Signal	Method	t_{ot}/s
B1C	General carrier loop	5.812 875
	Adaptive phase-frequency switching	4.266 694
B3I	General carrier loop	3.234 685
	Adaptive phase-frequency switching	2.527 196

As seen from Table 4, the adaptive phase-frequency switching method can greatly reduce the time consumption without losing the carrier tracking effect. For B1C signal, in contrast to the general carrier loop method, the proposed method can reduce the time consumption by 26.60%. Similarly, the proposed method can reduce the time consumption by 21.87% for B3I signal.

5 Conclusion

The acquisition and tracking method for the B1C and B3I bands of BDS-3 is proposed in this paper. The tracking results verify the availability of the proposed method. The acquisition and tracking of the new signals of Beidou-3 satellites is completed and then the navigation message can be demodulated according to the tracking results, which is vital to the commercial and civil use of BDS-3. The proposed method can be used for the B1C and B3I frequency bands of Beidou-3 satellites which have just been put into use. In addition, this study can also provide a theoretical basis for the use of BDS-3 which is forward-looking, practical and reliable. Future work will include BDS-3 B2a signal processing method and positioning algorithm using BDS-3.

References

[1] DING X C. Development of Beidou navigation satellite system [C]//*Proceedings of the 24th International Technical Meeting of the Satellite Division of the Institute of Navigation*. Portland, OR, USA: Oregon Convention Center, 2011: 882-912.

[2] YANG X, CHEN B. Beidou satellite navigation system enters a new era of global networking [J]. *Satellite Application*, 2017, **11**: 4 (in Chinese).

[3] XIN J. Research on GPS precise satellite clock bias prediction based on wavelet and spectral analysis [D]. Chengdu, China: Southwest Jiaotong University, 2016 (in Chinese).

[4] LUCAS-SABOLA V, SECO-GRANADOS G, LÓPEZ-SALCEDO J A, et al. Cloud GNSS receivers: New advanced applications made possible [C]//*2016 International Conference on Localization and GNSS* (*ICL-GNSS*). Barcelona, Spain: IEEE, 2016: 1-6.

[5] BETZ J W. Binary offset carrier modulations for radio navigation [J]. *Navigation*, 2001, **48**(4): 227-246.

[6] WU Z J. Data acquisition, research and analysis on Galileo E1 signal [D]. Shanghai, China: Shanghai Jiao Tong University, 2009 (in Chinese).

[7] FOUCRAS M, NGAYAP U, BACARD F, et al. Acquisition performance comparison of new generation of GNSS BOC-modulated signals [C]//*29th International Technical Meeting of the Satellite Division of the Institute of Navigation* (*ION GNSS+2016*). Portland, OR, USA: Institute of Navigation, 2016: 107-119.

[8] O'DRISCOLL C, RODRIGUEZ J Á Á, IOANNIDES R. Bandlimiting and dispersive effects on high order BOC signals [C]//*Proceedings of the 29th International Technical Meeting of the ION Satellite Division* (*ION GNSS+2016*). Portland, OR, USA: Institute of Navigation, 2016: 236-248.

[9] HE C L, WANG Y. Weil code correlation performance of GPS L1C signal [J]. *Radio Communication Technology*, 2013, **39**(1): 32-35 (in Chinese).

[10] MIRALLES D, HUARD J, AKOS D M, et al. FFT algorithms implementation for real-time GNSS receivers in embedded processors [C]//*Proceedings of the 29th International Technical Meeting of the ION Satellite Division* (*ION GNSS+2016*). Portland, OR, USA: Institute of Navigation, 2016: 62-69.

[11] VAN NEE D J R V, COENEN A J R M. New Fast GPS code-acquisition technique using FFT [J]. *Electronics Letters*, 1991, **27**(2): 158-160.

[12] FANTINO M, DOVIS F, PRESTI L L, et al. Acquisition performance analysis for BOC modulated signals [C]//*The 2004 International Symposium on GNSS/GPS*. Sydney, Australia: GNSS, 2004: 22832695

[13] LIU T M. Data research and analysis on B1 signal of BDS [D]. Shanghai, China: Shanghai Jiao Tong University, 2013 (in Chinese).

[14] LIANG C. Research on the modulation and synchronization of BOC navigation signal [D]. Guilin, China: Guilin University of Electronic Technology, 2014 (in Chinese).